ELSEVIER

Ceramics International 33 (2007) 1133–1136

CERAMICS INTERNATIONAL

www.elsevier.com/locate/ceramint

Short communication

Nitrate–citrate combustion synthesis of $Ce_{1-x}Gd_xO_{2-x/2}$ powder and its characterization

Cheng Peng *, Zhen Zhang

Department of Applied Chemistry, South China University of Technology, P.O. Box 85, Guangzhou 510640, PR China

Received 21 October 2005; received in revised form 18 December 2005; accepted 9 March 2006
Available online 23 June 2006

Abstract

The structure, thermal expansion coefficients, and electric conductivity of $Ce_{1-x}Gd_xO_{2-x/2}$ ($x = 0$–0.6) solid solution, prepared by the gel-combustion method, were investigated. The uniform small particle size of the gel-combustion prepared materials allows sintering into highly dense ceramic pellets at 1300 °C, a significantly lower temperature compared to that of 1600–1650 °C required for ceria solid electrolytes prepared by traditional solid state techniques. XRD showed that single-phase solid solutions formed in all the investigated range. The maximum conductivity, $\sigma_{600\,^\circ C} = 5.26 \times 10^{-3}$ S/cm, was found at $x = 0.2$. The thermal expansion coefficient, determined from high-temperature X-ray data, was $8.125 \times 10^{-6}\ K^{-1}$ at $x = 0.2$.

Keywords: Solid electrolyte; Combustion synthesis; Cerium oxide; Gadolinium oxide

1. Introduction

Solid oxide fuel cells (SOFC) attract widespread attention due to their high-energy conversion efficiency, fuel flexibility and environmental safety [1–3]. A typical SOFC which utilizes yttria-stabilized zirconia (YSZ) as the electrolyte requires high operated temperature, such as 1000 °C, to gain a high enough ionic conductivity. Lowering the operation temperature would prolong the lifetime of the cell and the SOFC stability, widen the selection of electrodes, interconnect and manifold materials and reduce the cost of material processing and cell fabrication [4,5]. As CeO_2-based solid electrolyte exhibits high ionic conductivity at intermediate temperature (600–800 °C), which is comparable with that of YSZ at high temperature, many researches have been focused on this system [6,7].

$(CeO_2)_{1-x}(GdO_{1.5})_x$ is a very promising material for use as an electrolyte in medium-temperature solid oxide fuel cell applications. For example, $(CeO_2)_{0.8}(GdO_{1.5})_{0.2}$ has been reported to have an ionic conductivity of ca. 0.1–0.2 S/cm at 800–850 °C [8–10]. Furthermore, Cho [11] found that Gd-doped CeO_2 improved oxygen storage. Doped ceria, however, is prone to electronic conductivity under reducing environments and high temperature due to the reduction of Ce^{4+} [12]. It has been reported by Riess [13] that the electronic contribution can be suppressed at sufficient high oxygen ion current density. Therefore, it will be a promising candidate as a solid electrolyte in SOFC which can be operated at intermediate temperature.

The majority of past work has been undertaken on doped ceria using traditional solid state techniques which has caused some troubles [14]. For example, theoretical densities are less than 95%. Moreover, the samples were sintered at 1600–1650 °C, which is costly and can allow ceria to be lost due to the high mobility of Ce^{4+} at these temperatures. Combustion synthesis is an important powder processing technique generally used to produce complex oxide ceramics [15–18]. The synthesized powders are generally more homogeneous, contain fewer impurities, and have higher surface areas than powders prepared by conventional solid state methods [19].

In this paper we present results of a systematic study of the structure, electrical conductivity and thermophysical properties of $Ce_{1-x}Gd_xO_{2-x/2}$ ($x = 0$–0.6) solid solution prepared by the gel-combustion method.

2. Experimental

According to the stoichiometric ratios of $Ce_{1-x}Gd_xO_{2-x/2}$, $Ce(NO_3)_3$ and $Gd(NO_3)_3$ solutions were mixed, citric acid was

* Corresponding author.
E-mail address: chengpen@scut.edu.cn (C. Peng).

0272-8842/$32.00
doi:10.1016/j.ceramint.2006.03.004

then added in a proportion of 2 mol/mol of metal atom and the pH of the solution was adjusted to ≈8 by adding ammonium hydroxide. The solution was vaporized on water bath at 60–70 °C and finally it became a transparent gel. The resulting gel was heated on a hot plate until it turned into a black viscous mass, which on continued heating burned due to a vigorous exothermic reaction. Shallow-yellowish ashes obtained after combustion were treated at 500 °C in muffle furnace. The product was pressed into pellets. Finally, the pellets were sintered at 1300 °C for 10 h in furnace and cooled to room temperature.

The thermal decomposition in the air of the dried gel precursor was investigated by means of differential thermal analysis (DTA) and thermogravimetric analysis (TGA), which were carried out in the temperature range 25–800 °C with Shimadzu DT-30B with a heating rate of 10 °C/min in an oxidizing atmosphere (N_2 + 21% O_2, flow rate 50 ml/min).

The room temperature powder X-ray diffraction patterns of the ultrafine powders were obtained with Rigaku D/Max-IIB X-ray diffractometer with Cu $K\alpha_1$ radiation at a 2θ scan of 1° min^{-1}. High temperature X-ray diffraction was carried out on MAC MXP[18] diffractometer using Cu $K\alpha_1$ radiation. Data were collected in the 2θ range from 20° to 100°. Cell parameters were calculated by CELL program [20]. The reflection from the (1 1 1) plane was used for the determination of average crystallite size. The average crystallite size, D, of the prepared powder was calculated from the Scherrer formula: $D = 0.9\lambda/\beta \cos\theta$, where λ is the wavelength of the X-rays, θ the diffraction angle, $\beta = (\beta_m^2 - \beta_s^2)^{1/2}$ the corrected halfwidth of the observed halfwidth, β_m, of the (1 1 1) reflection in samples of $Ce_{1-x}Gd_xO_{2-x/2}$, and β_s is the halfwidth of the (1 1 1) reflection in a standard sample of CeO_2 ($D \sim 100$ nm).

The sintered pellets were coated with platinum by a SC-701 QUICK COATER. The electrical conductivity of the coated pellets were measured at different temperatures using a Solartron 1255 hf frequency response analyzer and the 1287 electrochemical interface operating in the frequency range of 0.1–1 MHz.

3. Results and discussion

Fig. 1 shows simultaneous TGA and DTA plots obtained for the dried gel. As can be seen in the DTA plot, there exists a weak endothermic peak and a strong one near 135 °C and 170 °C, respectively. Then around 284 °C a weak exothermic peak appeared and after that a strong one emerged near 350 °C. Accompanied by the change of DTA, TGA curve shows that the sample lost weight gradually below 450 °C. The first endothermic peak with 11% weight loss could be attributed primarily to the dehydration of gel and the second one with 44% weight loss accounted for the thermal decomposition of it. Meanwhile, the two pronounced exothermic peaks appearing in the DTA probably corresponded to the burning course of the residual organic matter in the sample and to the gradually crystallization process of $Ce_{0.8}Gd_{0.2}O_{2-\delta}$. Furthermore, it was observed by DTA measurements that the base line of the DTA curve deviates to the endothermic side at a temperature near

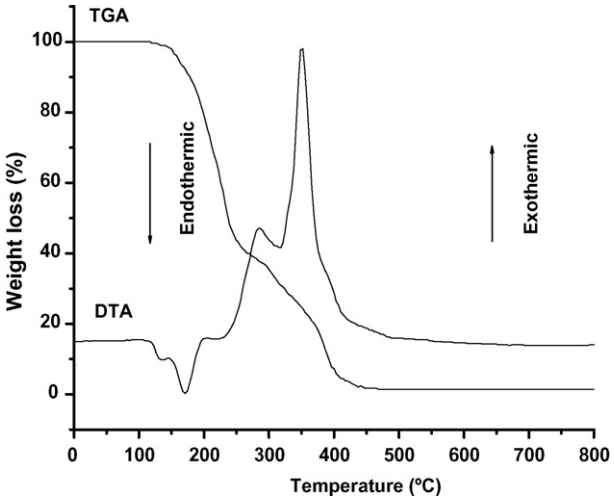

Fig. 1. DTA and TGA curves of the dried precursor gel.

500 °C. This suggests an increase of the specific heat of the compounds. This increase does not necessarily mean the existence of transition in the crystal lattice, because X-ray measurement revealed no pattern change happened between lower and higher temperatures.

In order to compare with DTA/TGA data, the fluorite-phase evolution during the gel-combustion process as a function of heat-treatment temperature was examined by XRD for $Ce_{0.8}Gd_{0.2}O_{2-\delta}$ and the results are shown in Fig. 2. No evidence of impurity was observed at 160 °C. The XRD pattern is that of pure CeO_2, however, the peak was wider and the intensity was weaker, compared to that of pure CeO_2. This suggests that at such low heat-treatment temperature, which is significantly lower of the traditional solid state technique [21], the samples can form cubic fluorite structure. It is evident from Fig. 2 that with increasing heat-treatment temperature the halfwidth of peaks became narrower and the intensity of them got stronger.

The lattice parameter, average crystallite size, and apparent density of $Ce_{1-x}Gd_xO_{2-x/2}$ are summarized in Table 1. The

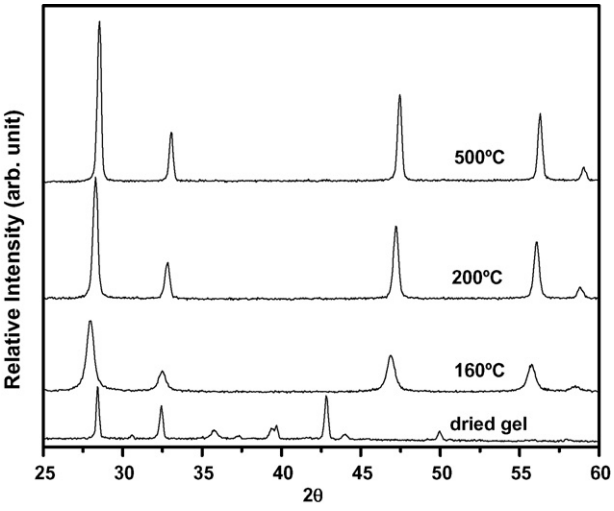

Fig. 2. Thermal evolution of the powder X-ray diffraction spectrum of $Ce_{0.8}Gd_{0.2}O_{2-\delta}$ powder.

Table 1
Lattice parameter, crystallite size and density of specimens used in this study

Composition, x	Lattice parameter, a (nm)	Average crystallite size D (nm)	Percentage theoretical density (%)
0.1	0.54213	28.00	95.27
0.2	0.54302	11.00	95.99
0.3	0.54310	19.00	96.28
0.4	0.54449	24.00	96.48
0.5	0.54481	28.00	95.49
0.6	0.54431	28.00	95.21

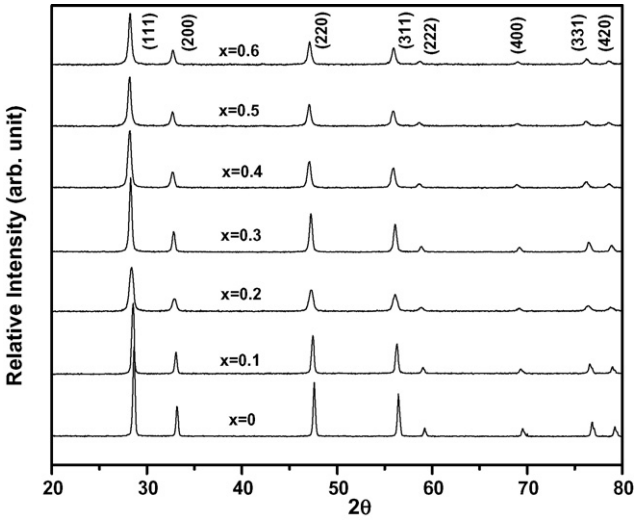

Fig. 3. Powder X-ray diffraction patterns of $Ce_{1-x}Gd_xO_{2-x/2}$ solid solutions.

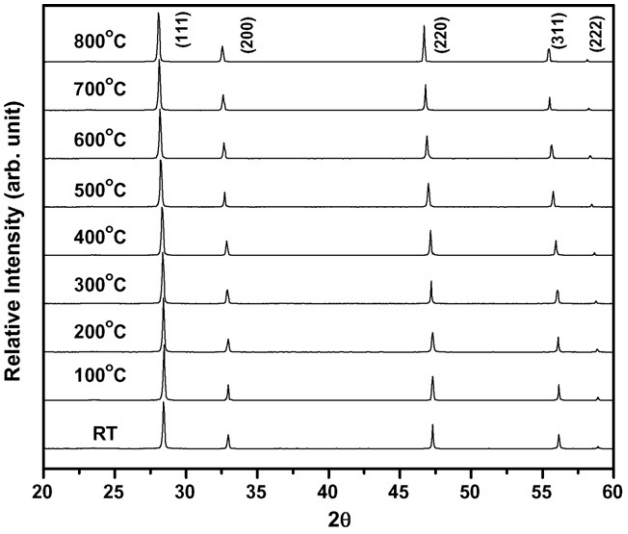

Fig. 5. High temperature PXD patterns of $Ce_{0.8}Gd_{0.2}O_{2-\delta}$ powder.

average crystallite size, D, of gadolinium substituted ceria powders, calculated by the Scherrer formula from the XRD data was between 11 and 28 nm (Table 1). The ultrafine substituted ceria powders were sintered into pellets at 1300 °C with apparent densities of over 95% of the theoretical value, while ceria solid electrolytes prepared by conventional ceramic techniques require over 1600 °C for sintering.

Fig. 3 shows the X-ray diffraction patterns of $Ce_{1-x}Gd_xO_{2-x/2}$ systems, all of which are similar to that of the fluorite-type structure of CeO_2. Furthermore, no impurity is observed up to $x = 0.6$. We have calculated its crystal structure using CELL program. The results indicated that all the samples can be indexed according to a cubic structure. Fig. 4 shows the change of the calculated cell parameter and unit volume with the substitution x. The lattice parameter and unit volume increased steadily at $x < 0.4$, reached the maximum at $x = 0.5$ and gradually decrease at $x > 0.5$ (Fig. 4). Bevan et al. [22] interpreted that this saturation is due to the Gd^{3+} ions and oxygen vacancies strong interaction. As the fluorite lattice and the C-type Gd_2O_3 give quite similar X-ray diffraction patterns, it is difficult to determine the solubility limit precisely by this

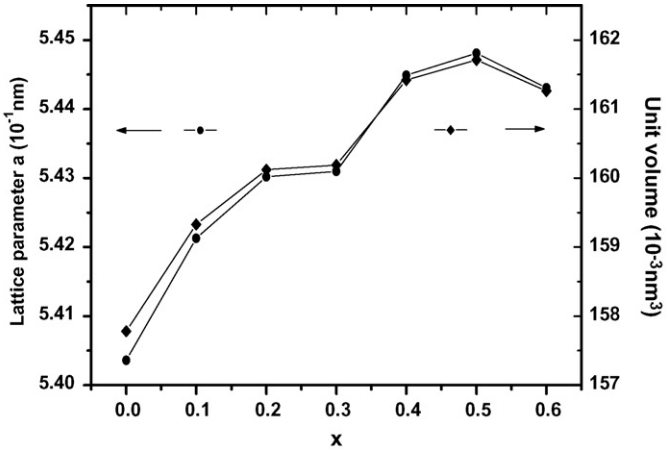

Fig. 4. Lattice parameter and unit volume of $Ce_{1-x}Gd_xO_{2-x/2}$ solid solutions as a function of x.

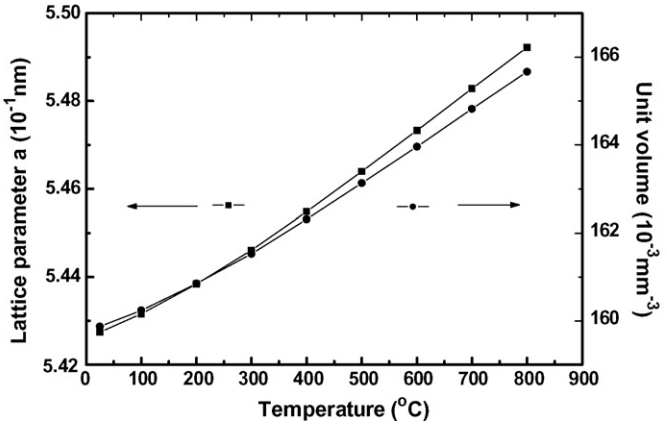

Fig. 6. Temperature dependence of the lattice parameter and unit volume of $Ce_{0.8}Gd_{0.2}O_{2-\delta}$ powder.

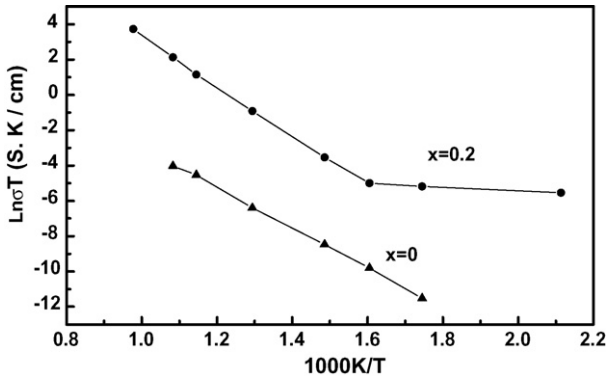

Fig. 7. Arrhenius plots of the ionic conductivity of $Ce_{0.8}Gd_{0.2}O_{2-\delta}$ solid solution.

method. The increase in lattice constant and unit cell volume indicates the dissolution of the Gd_2O_3 in the fluorite lattice. In addition, as evident in Fig. 4, the lattice expansion agreed perfectly with effective ionic radii considerations ($r_{Gd^{3+}} = 0.1193$ nm, $r_{Ce^{4+}} = 0.1110$ nm) [23].

The high temperature crystal structure was investigated by high temperature X-ray diffraction of the $Ce_{0.8}Gd_{0.2}O_{2-\delta}$ powder (Fig. 5) which revealed that no phase transition occurred from room temperature to 800 °C and all diffraction peaks systematically shifted to lower angles with increasing temperature. Evaluation of the XRD patterns taken at different temperatures using the CELL program indicated all samples to have a cubic structure with S.G. *Fm*3*m*. Fig. 6 presents the temperature dependence of the lattice parameter and unit volume of the $Ce_{0.8}Gd_{0.2}O_{2-\delta}$ powder. It is seen from Fig. 6 that the unit cell parameter and unit volume increased almost linearly with temperature. In addition, the thermal expansion coefficient determined from Fig. 6 is $8.125 \times 10^{-6}\,K^{-1}$.

Fig. 7 presents an Arrhenius plot for the compound $Ce_{0.8}Gd_{0.2}O_{2-\delta}$. This graph can well be approximated by two linear lines, which suggests that the oxygen ion transport mechanism in this electrolyte seems to change at about 350 °C, giving different activation energies in the two regions. At temperature lower than 350 °C, the sample showed a lower activation energy. But after that, higher activation energy appeared. The reason for this trend is not very fully clear at present and will be the subject of further investigation. As mentioned above, DTA measurement suggests an increase of the specific heat of the compound near 500 °C. It seems likely that at this temperature some higher order transition occurs. This probably is the reason for the existence of two regions in the Arrhenius plot. In addition, a close inspection of Fig. 7 shows ionic conductivity to be significantly enhanced in the $Ce_{0.8}Gd_{0.2}O_{2-\delta}$ solid electrolyte compared to pure ceria by increasing the oxygen vacancies $V_0^{\bullet\bullet}$: $2CeO_2 \rightarrow 2Gd_{Ce}' + V_0^{\bullet\bullet} + 1/2O_2$. It was found that the ionic conductivity of $Ce_{1-x}Gd_xO_{2-x/2}$ increases systematically with increasing Gd substitution and reaches a maximum for the composition $Ce_{0.8}Gd_{0.2}O_{2-\delta}$.

4. Conclusions

$Ce_{1-x}Gd_xO_{2-x/2}$ ($x = 0$–0.6) solid solutions with the fluorite structure were prepared by the gel-combustion method. Ultrafine particles with size of 11–28 nm were formed. Because of the small particle size of the doped ceria, the sintering temperature needed to obtain a dense ceramic pellet was reduced substantially from 1600 °C, which is required for the corresponding materials prepared by conventional solid state methods, to ~1300 °C. High temperature X-ray diffraction measurements showed that no phase transition happened from room temperature to 800 °C in the $Ce_{0.8}Gd_{0.2}O_{2-\delta}$ sample. The highest conductivity was found for the $x = 0.2$ Gd substituted ceria ($\sigma_{600\ ^\circ C} = 5.26 \times 10^{-3}$ S/cm).

Acknowledgement

The author gratefully acknowledges the financial support of the Nature Science Young Teacher Fund of South China University of Technology (No. B15-E5050650).

References

[1] O. Yamamoto, Electrochim. Acta. 45 (2000) 2423.
[2] B.C.H. Steele, J. Mater. Sci. 36 (2001) 1053.
[3] V.V. Kharton, A.P. Viskup, I.P. Marozau, E.N. Naumovich, Mater. Lett. 57 (2003) 3017.
[4] A. Boudghene Stambouli, E. Traversa, Renewable Sustainable Energy Rev. 6 (2002) 433.
[5] W. Huang, P. Shuk, M. Greenblatt, Solid State Ionics 100 (1997) 23.
[6] D.Y. Chung, E.H. Lee, J. Alloys Compd. 374 (2004) 69.
[7] Y.P. Fu, C.H. Lin, J. Alloys Compd. 389 (2005) 165.
[8] N.Q. Minh, J. Am. Ceram. Soc. 76 (1993) 563.
[9] G.M. Christie, F.P.F. van Berkel, Solid State Ionics 83 (1996) 17.
[10] J.M. Ralph, J.A. Kilner, U. Stimming, S.C. Singhal, H. Tagawa, W. Lehnert (Eds.), Solid Oxide Fuel Cells, vol. V, The Electrochemical Society, Pennington, NJ, 1997, p. 1105.
[11] B.K. Cho, J. Catal. 131 (1991) 74.
[12] H. Yahiro, Y. Baba, K. Eguchi, H. Arai, J. Electrochem. Soc. 135 (1988) 2077.
[13] I. Riess, Solid State Ionics 52 (1992) 127.
[14] L.E. Shea, J. McKittrick, O.A. Lopez, J. Am. Ceram. Soc. 79 (12) (1996) 3257.
[15] J. Poth, R. Haberkorn, H.P. Beck, J. Eur. Ceram. Soc. 20 (2000) 707.
[16] A.S. Mukasyan, C. Costello, K.P. Sherlock, D. Lafarga, A. Varma, Sep. Purif. Technol. 25 (2001) 117.
[17] S. Arul Antony, K.S. Nagaraja, O.M. Sreedharan, J. Nucl. Mater. 295 (2001) 189.
[18] L.B. Fraigi, D.G. Lamas, N.E. Walsoe de Reca, Mater. Lett. 47 (2001) 262.
[19] J.J. Kingsley, L.R. Pederson, Mater. Res. Soc. Symp. Proc. 296 (1993) 361.
[20] Y. Takaki, T. Taniguchi, K. Nakata, H. Yamaguchi, Program for finding the unit-cell constants and the space group from X-ray powder diffraction data—the case where approximate unit-cell constants are known, J. Ceram. Soc. Jpn. 97 (1989) 763.
[21] R.T. Dirstine, R.N. Blumenthal, T.F. Kuech, J. Electrochem. Soc. 126 (1979) 264–269.
[22] D.J.M. Bevan, W.W. Barker, R.L. S Martin, in: L. Eyring (Ed.), Proceedings of the 4th Conference on Rare Earth Research, Phoenix, AZ, 1964, Gordon and Breach, New York, (1965), p. 441.
[23] R.D. Shannon, Acta Cryst. A32 (1976) 751.